Available online at www.sciencedirect.com
ScienceDirect
Journal of the European Ceramic Society 28 (2008) 2933–2939
www.elsevier.com/locate/jeurceramsoc

Densification and grain growth of nanocrystalline 3Y-TZP during two-step sintering

Mehdi Mazaheri [a], A. Simchi [a,b,*], F. Golestani-Fard [c]

[a] Department of Materials Science and Engineering, Sharif University of Technology, P.O. Box 11365-9466, Azadi Avenue, 14588 Tehran, Iran
[b] Institute for Nanoscience and Nanotechnology, Sharif University of Technology, P.O. Box 11365-9466, Azadi Avenue, 14588 Tehran, Iran
[c] Department of Materials and Metallurgical Engineering, Iran University of Science and Technology, Tehran, Iran

Received 2 February 2008; received in revised form 26 April 2008; accepted 26 April 2008
Available online 18 June 2008

Abstract

Two-step sintering (TSS) was applied on nanocrystalline yttria tetragonal stabilized zirconia (3Y-TZP) to control the grain growth during the final stage of sintering. The process involves firing at a high temperature (T1) followed by rapid cooling to a lower temperature (T2) and soaking for a prolonged time (t). It is shown that for nanocrystalline 3Y-TZP (27 nm) the optimum processing condition is T1 = 1300 °C, T2 = 1150 °C and t = 30 h. Firing at T1 for 1 min yields 0.83 fractional density and renders pores unstable, leading to further densification at the lower temperature (T2) without remarkable grain growth. Consequently, full density zirconia ceramic with an average grain size of 110 nm is obtained. XRD analysis indicated that the ceramic is fully stabilized. Single-step sintering of the ceramic compact yields grain size of 275 nm with approximately 3 wt.% monoclinic phase. This observation indicates that at a critical grain size lower than 275 nm, phase stabilization is induced by the ultrafine grain structure.

Keywords: Nanocrystalline 3Y-TZP; Two-step sintering; Densification; Grain growth

1. Introduction

Yttria stabilized zirconia ceramics display high fracture toughness that makes them suitable for a wide range of structural applications such as cutting tools, valve guides, extrusion dies, abrasive tools, etc.[1,2] It has recently been shown that superplastic deformation and higher hardness are gained when an ultrafine-grained toughened ceramics are utilized.[3] Meanwhile, further improvement in the properties is expected by decreasing the grain size reduce to nano-scale.[4] Although the sinterability of nanoparticles is superior to fine particles due to higher sintering stresses, the more intensive grain growth during densification deteriorates the advantages of nanostructured bulk materials.[5] Spark plasma sintering (SPS) and hot pressing are two key techniques to produce nanostructured ceramics.[6,7] These methods yield a rapid sintering rate, high density and ultrafine grain structure. However, limitations such as production cost, shape-complexity, and product size might exist dependent on the particular material and application.[8,9]

It is known that, the grain growth during pressureless sintering depends on the shaping method and firing temperature. By the wet shaping methods, e.g. slip and gel casting, Krell and Blank[10] have produced green parts with narrow size pores which can easily be eliminated upon final stage sintering. Duran et al.[11] have used this procedure to produce dense Y-TZP nanostructured ceramic by conventional sintering at 1070 °C.

Recently, Chen and Wang[12] have developed a new technique called two-step sintering (TSS) for Y_2O_3 which is a promising approach to obtain fully dense nano-grained ceramics. The key elements in this method are[13]: (I) heating to a high temperature (T1) to conduct first step sintering and to achieve a critical density (ρ^*) to render the pores unstable; (II) decreasing the temperature (T2) to conduct sintering without any grain growth at the lower temperature. Besides Y_2O_3, TSS has been successfully applied to ZnO,[14] Ni–Cu–Zn ferrite,[15] $BaTiO_3$[15] and Al_2O_3.[16] The liquid phase sintering of SiC[17] and doped ZnO varistors[18]

* Corresponding author at: Department of Materials Science and Engineering, Sharif University of Technology, P.O. Box 11365-9466, Azadi Avenue, 14588 Tehran, Iran. Tel.: +98 21 6616 5262; fax: +98 21 6616 5261.
E-mail address: simchi@sharif.edu (A. Simchi).

0955-2219/$ – see front matter © 2008 Elsevier Ltd. All rights reserved.
doi:10.1016/j.jeurceramsoc.2008.04.030

has also been reported. Yu et al.[19] used this technique to control the grain growth of YSZ ceramic by powder injection molding (PIM). Although high density parts were produced, no effect of the sintering temperature on the final grain size was determined. The advantages of TSS method for injection-molded 3Y-TZP submicron powder has also been shown by Lee.[20]

To further study the effect of TSS on the densification and grain growth of nanocrystalline 3Y-TZP, different TSS regimes are designed and applied to 3Y-TZP (27 nm) compacts. The temperature range in which the residual porosity can be eliminated without the final stage of grain growth is determined. The effect of sintering cycle on the densification and grain growth is addressed. A comparison is made with the conventional sintering procedure.

2. Experimental procedure

ZrO_2–3 mol% Y_2O_3 powder was supplied from Tosoh Co. (Tokyo, Japan). The powder composed of spherical granules (Fig. 1a) with primary particles with an average size of ~75 nm (Fig. 1b). The specific surface area of the powder was determined by Brunauer–Emmett–Teller (BET) technique (Micromeretics Gemini 2375, USA) and found to be 17.2 $m^2\,g^{-1}$. The X-ray diffraction (XRD) pattern of the powder taken by Cu Kα radiation (Philips PW3710, Netherlands) is shown in Fig. 2. The average crystallite size was determined by Scherrer equation[21] and found to be 27 nm, which is in agreement with the results of others.[22] The weight fraction of the monoclinic phase, X_m, was calculated using the following equation[23]:

$$X_m = \frac{I(1\,1\,\bar{1})_m + I(1\,1\,1)_m}{I(1\,1\,\bar{1})_m + I(1\,1\,1)_m + I(1\,1\,1)_t} \quad (1)$$

where $I(1\,1\,1)_m$, $I(1\,1\,\bar{1})_m$ and $I(1\,1\,1)_t$ are the integrated intensity from the monoclinic (1 1 1), monoclinic (1 1 $\bar{1}$) and the tetragonal (1 1 1) peaks, respectively. The powder composed of 23 wt.% monoclinic phase and 77 wt.% tetragonal phase.

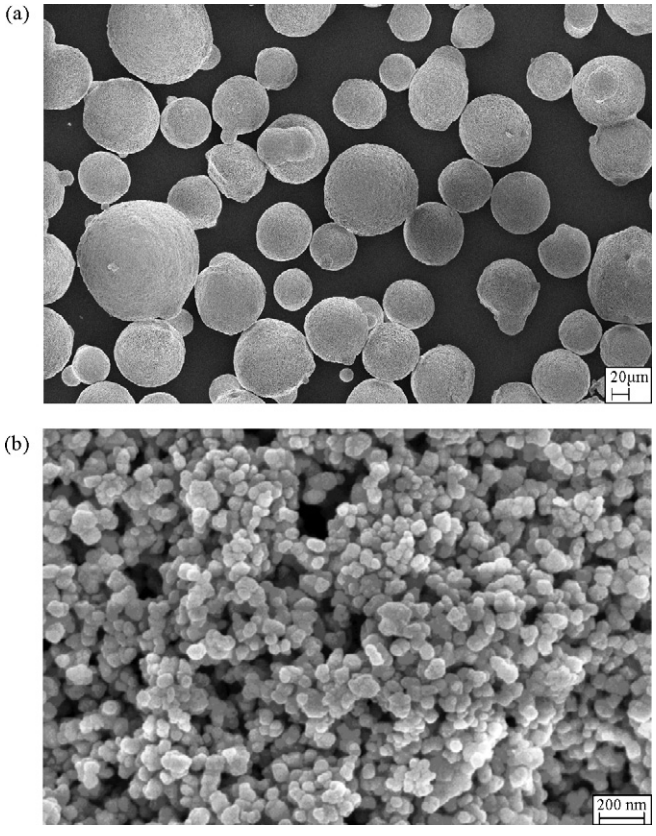

Fig. 1. SEM micrographs show the particle morphology of 3Y-TZP: (a) spray-dried granules; (b) primary particles.

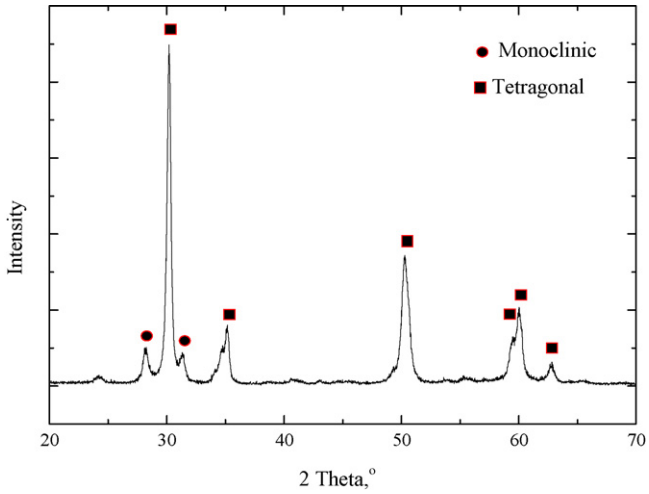

Fig. 2. X-ray diffraction pattern of nanocrystalline 3Y-TZP powder.

The powder was compacted in a cylindrical die at 150 MPa to produce green compacts with 10 mm diameter and 3 mm height. The green density was ~45% of the pore free density. A TMA 801 sinter-dilatometer (NETZCH, Germany) was used to study the nonisothermal sintering behavior of the powder compacts. The heating rate to the sintering temperature was 5 °C min^{-1}. The relative density of the sintered specimen (ρ_s) was calculated using the following equation instantaneously[23]:

$$\rho_s = \left[\frac{1}{1 - dL/L_0 + \alpha(T - T_0)}\right]^3 \rho_g \quad (2)$$

where dL/L_0 is instantaneous liner shrinkage obtained by the dilatometer test, L_0 is the initial length of the specimen, ρ_g is the green density, T_0 is the room temperature, and α is the coefficient of thermal expansion.

Single-step sintering (SSS) was carried out at 1100–1500 °C in air with 50 °C temperature intervals. The heating rate was 5 °C min^{-1}. The dwell time varied between 1 and 8 h. For the binder removal, 0.5 h soak at 500 °C was applied. Five different two-step sintering cycles were used (Table 1). The compacts were heated to T1 at the rate of 5 °C min^{-1} after de-lubrication at 500 °C for 0.5 h. A dwell time of 1 min was given. The specimens were the cooled to T2 with a rate of 50 °C min^{-1}. Up to 30 h dwell time was tested for sintering at T2.

The density of the sintered sample was measured by the water displacement (Archimedes) method according to ISO Standard 39231/1-1979(E). Microstructure of the sintered compacts was observed by SEM (Philips XL30, Netherlands) after sequential mechanical polishing using diamond pastes (3, 1 and 0.05 μm)

Table 1
Two-step sintering cycles used in the present work

Regime	T_1 (°C)	t_1[a] (min)	T_2 (°C)	t_2[b] (h)
TSS1	1350	1	1150	2–5–8–12–15–20
TSS2	1250	1	1150	2–5–8–12–15–20
TSS3	1300	1	1150	2–5–8–12–15–20–25–30
TSS4	1300	1	1250	2–5–8–12–15–20
TSS5	1300	1	1050	2–5–8–12–15–20–25–30

[a] Holding time at T_1.
[b] Holding time at T_2.

and thermal etching at 50 °C below the sintering temperature. The average grain size of the sintered compacts was determined by the linear intercept method (ASTM Standard E112). For each specimen, 15 line segments were considered and Mendelson[24] multiplying factor (1.56) was used. The phase constitution of sintered compacts was evaluated by XRD method as described above. Here, a high-resolution scan over the range 25–35° with a step size of 0.01° and scan speed of 0.002° s^{-1} was performed.

3. Results and discussion

Fig. 3 shows shrinkage and shrinkage rate of 3Y-TZP compact during nonisothermal sintering at heating rate of 5 °C min^{-1}. Sintering shrinkage (0.5%) started at 961 °C and the maximum shrinkage rate occurred at 1255 °C. The amount of shrinkage at 1255 °C was 16.6% and reached to 21.6% at 1300 °C. The shrinkage rate peak of the dilatometric curve can be an indication of the homogeneous porosity distribution in the green compacts.[25] As it has been reported in[25,26] the presence of two shrinkage rate peaks might be attributed to sintering within and in between the hard agglomerate. This observation is important because several studies[25,27] have shown the difficulty in sintering of nanometric zirconia ceramic to full density at low temperatures due to hard agglomerates. In fact, when small primary particles are irreversibly bonded to as larger agglomerates, the advantages of the smaller particles are lost and the sintering behavior is determined solely by a larger agglomerate size.[5]

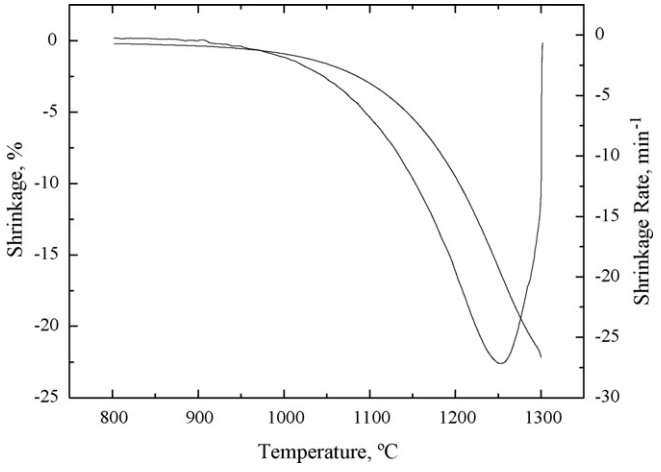

Fig. 3. The shrinkage and shrinkage rate profile of nanocrystalline 3Y-TZP powder compact.

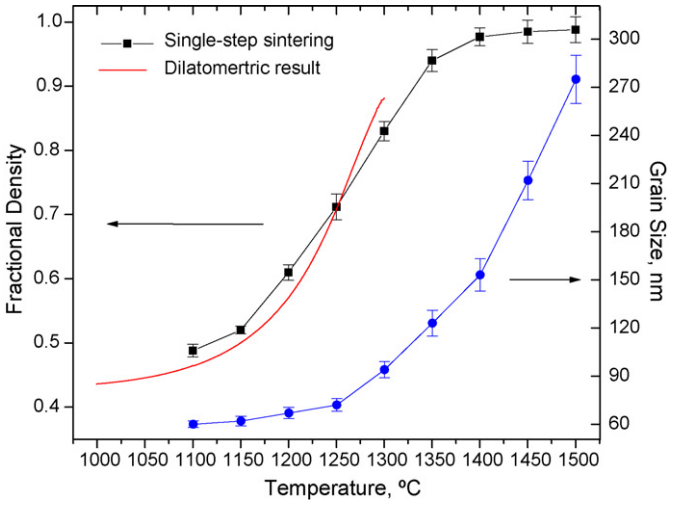

Fig. 4. Density and grain size of nanocrystalline 3Y-TZP compacts after single-step sintering at various temperatures for 1 min. The heating rate was 5 °C min^{-1}. The dilatometric data are included in the graph for comparison.

Fig. 4 shows the effect of sintering temperature on the densification and grain growth of the compacts sintered in the temperature range of 1100–1500 °C for 1 min. The results of the nonisothermal sintering are included for comparison. The variation of the density versus temperature exhibits a sigmoidal shape in the range of 1150–1350 °C. No significant densification was observed below 1100 °C. In the temperature range of 1150–1300 °C, the densification was accelerated without significant grain growth. At the higher temperature, however, the densification was marginal but the grain growth was fast (Fig. 5). For instance, while the fractional density increased from 0.977 to 0.988 with increasing the temperature from 1400 to 1500 °C, the average grain size became coarser from 153 to 275 nm. Fig. 6a and b shows SEM micrograph of conventionally sintered samples (SSS) at 1200 and 1400 °C. Many studies[14,16,27,28] have shown that dispersed open pores can pin grain boundaries and

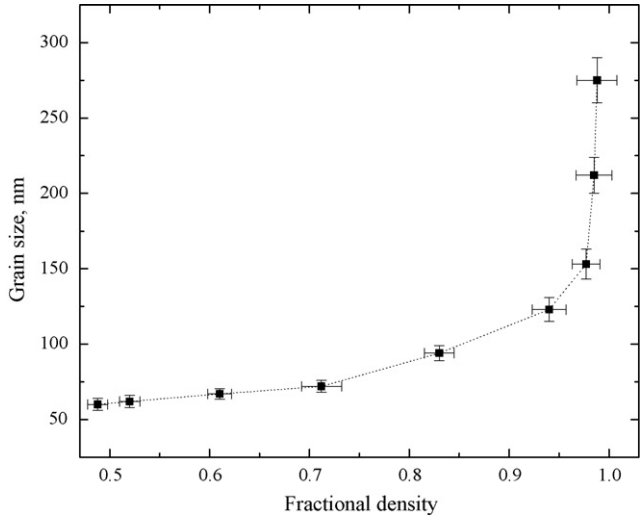

Fig. 5. The average grain size of 3Y-TZP versus the fractional density. The ceramic compacts were fired at various temperatures (1100–1500 °C) according to the single-step sintering cycle.

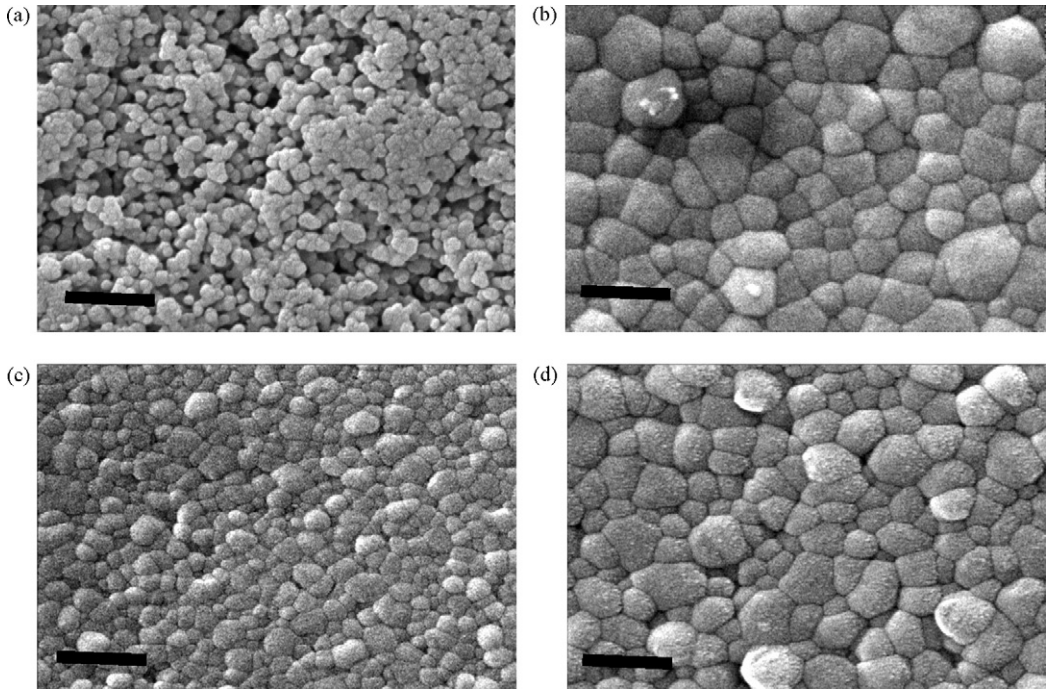

Fig. 6. SEM micrographs show the grain structure of 3Y-TZP compacts sintered under (a) SSS condition at 1200 °C, (b) SSS condition at 1400 °C, (c) TSS3 condition up to 30 h, and (d) TSS4 condition up to 12 h. The scale bar is 500 nm.

hinder grain-boundary migration at intermediate stage of sintering. At the final stage of sintering, when closed and small pores are formed, microstructural coarsening occurs. In fact, the collapse of open pores results in a substantial decrease in pore pinning, which triggers the accelerated grain growth. Nevertheless, it is noteworthy that as compared with other nanocrystalline ceramics such as ZnO[14] and Al_2O_3,[10] the grain growth rate of 3Y-TZP is limited. Gao and Li[29] and Mazaheri et al.[30] have reported a solid-solution drag-controlled grain growth mechanism, owing to the enrichment of Y^+ on the grain boundaries which hinders the grain growth.

Fig. 7 shows the variation of density and average grain size of the compacts sintered under different TSS conditions (Table 1) as a function of the dwell time at T2. The effect of different TSS cycles on the grain growth during TSS is shown in Fig. 8. To highlight the effect of TSS cycles, the results of SSS are included in the graph. TSS1 schedule conducted under T1 = 1350 °C and T2 = 1150 °C. The fractional density (ρ_1) after 1 min sintering at 1350 °C was 0.94 (Fig. 4). By firing at 1150 °C for 25 h, the density approached ~0.99 (Fig. 7a). The variation of the grain size versus the sintering time at T2 indicates no significant grain growth up to 12 h, although the fractional density was higher than 0.94. This observation suggests an incubation time for grain growth during two-step sintering.[13] Increasing the dwell time resulted in significant grain growth, particularly after 20 h holding. As it is appeared in Fig. 7, TSS1 succeeded to inhibit the grain growth at the final stage of sintering between 0.94 and 0.97. However, a full densification could not be obtained without remarkable grain growth, although the final grain size is smaller than that of SSS. Typically, parabolic growth at the end of TSS regime is related to the density of triple-point junction (three-grain junction-lines or four-grain junction-points).[14] At densities higher than a critical value, the density of the triple-point junction decrease. Under this circumstance, the effect of triple-point drag-mechanism was wasted to control the grain growth at the end of sintering process.[13] Therefore, a high density of triple-point junctions is required to suppress the grain growth. Shorter incubation time (12 h) should thus be obtained in order to attain full density without significant grain growth. For this aim, TSS2 cycle was conducted at T1 = 1250 °C and T2 = 1150 °C. As seen in Fig. 7b, no significant densification was obtained although the grains grew remarkably. Even after 30 h holding at 1150 °C, the fractional density reached 0.73 while the average grain size was 110 nm. This observation suggests that, to making the pores unstable it is inevitable to attain a critical density (ρ^*) after sintering at T1. Chen and Wang[12] have shown that the critical density (ρ^*) is greater than 0.75 for Y_2O_3. Bodisova and Sajgalik[16] and Li and Ye[31] have reported values of 0.92% and 0.82 for nanometric and submicron particles of alumina, respectively. Mazaheri et al. have shown this value was 0.78 for nanocrystalline ZnO.[14] The low value of density at the end of the first step implies that surface diffusion would still be active which can contribute to the neck growth and grain growth without significant influence on the shrinkage.[32] Based on the results of SSS, T1 was selected at 1300 °C to obtain the fractional density of 0.83. We will latter show that this density is enough to make pores unstable during the second sintering step at T2 with retarded grain growth by the triple-point junctions.

Further study was concentrated on changing T2. Cycle TSS3 was conducted at T2 = 1150 °C for various dwell time. Fig. 7c shows the results of density and grain size measurements. In contrast to TSS1 and TSS2 cycles, remarkable densification without significant grain growth was obtained (Fig. 8). Fig. 6c shows SEM micrograph of sintered samples under TSS3 condition for

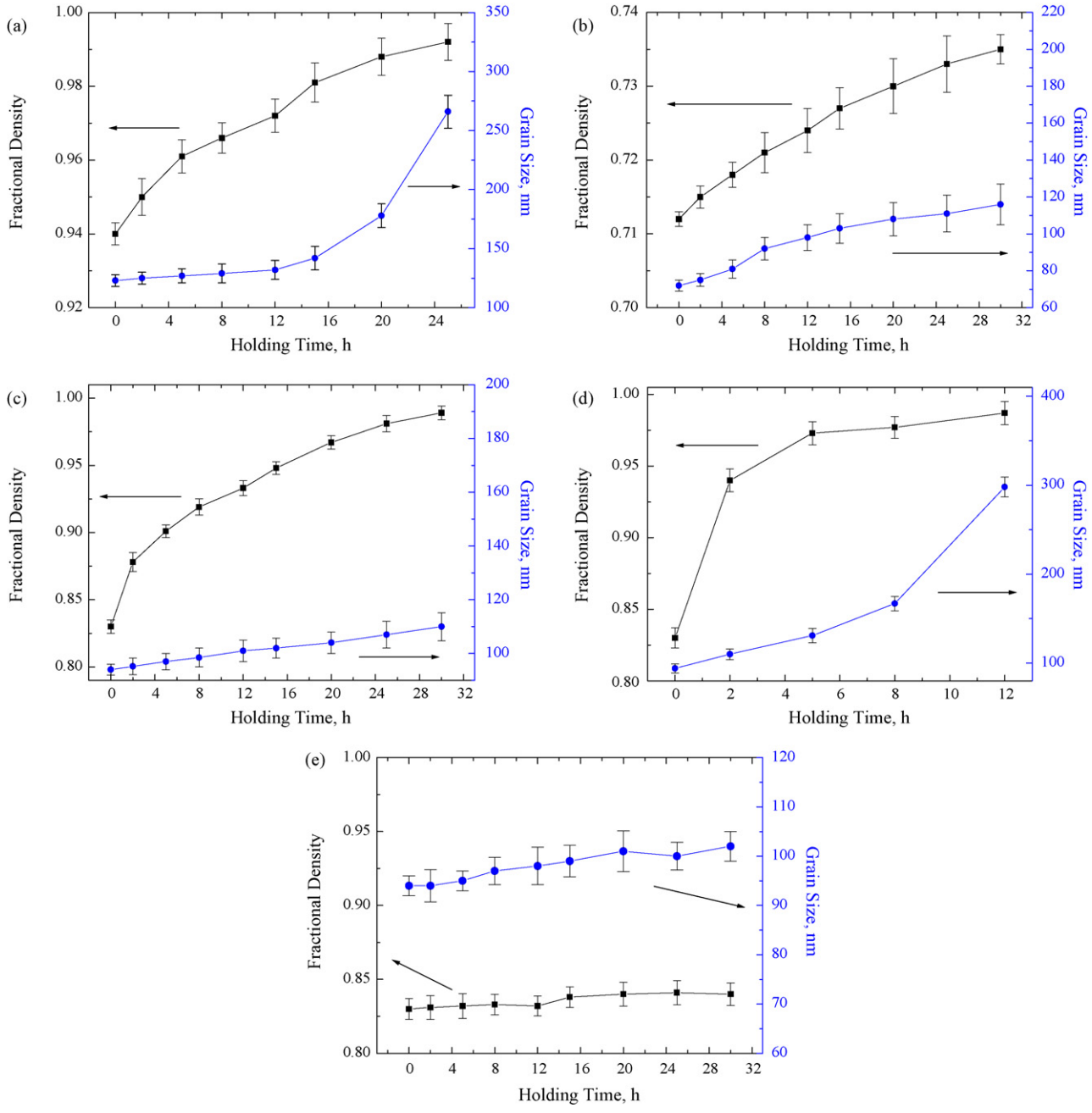

Fig. 7. Effect of dwell time on the density and grain size of 3Y-TZP compacts after two-step sintering: (a) TSS1; (b) TSS2; (c) TSS3; (d) TSS4; (e) TSS5.

30 h. The fractional density and average grain size is 0.989 and 110 nm, respectively. It appears that TSS3 cycle yields a near fully dense microstructure with a slow grain growth rate. Here, the grain-boundary diffusion should be active while the grain-boundary migration is suppressed. The mechanism for inhibiting the grain-boundary movement is triple-point (junction) drag.[13] In fact, at the low temperature the grain-boundary mobility is marginal because the triple junctions control the grain growth. The low sintering temperature also leads to a reduced entrapped gas pressure within the micropores. This can affect the densification because less resistance by the gas pressure against the matter transport may encourage the sintering process in the forward direction.[27]

To further study the effect of TSS on the densification and grain growth of the nanocrystalline 3Y-TZP powder compact, two other cycles were applied. In the both cycles, T1 was set at 1300 °C but T2 was changed to 1250 °C (TSS4) and 1050 °C (TSS5). The aim was to study the effect of temperature on the microstructural development. Fig. 7d shows the results for TSS4. As seen, the higher T2 temperature compared with TSS3 led to decreasing of the dwell time for achieving a high density. For instance, to attain the fractional density of 0.98 the holding time can be decreased from 30 to 8 h. Nevertheless, coarser grain structure was obtained (Fig. 6d). No incubation time for the grain growth is also noticeable. Apparently, the effect of TSS is diminished when close T2 and T1 temperatures are cho-

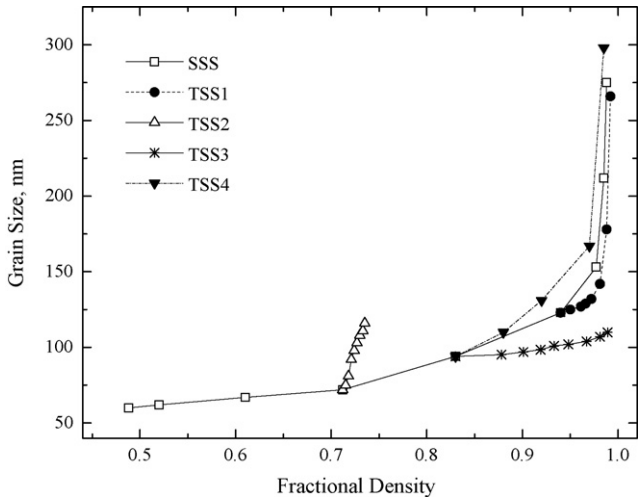

Fig. 8. Effect of firing cycle on the sintering path (grain size/fractional density) of 3Y-TZP.

sen. For better depiction of the results, the sintering path (grain size/fractional density trajectory) of TTS4 cycle is compared with SSS in Fig. 9. The results of conventional sintering at 1250 and 1300 °C for different holding time up to 8 h are also presented. No remarkable difference between different cycles can be identified. It appears that, if the temperature of the second stage (T2) is high enough to make grain boundaries and junctions mobile, the triple-point drag-mechanism will be unable to suppress the grain coarsening. On the other hand, a low T2 temperature (Fig. 7e), the densification and grain growth became very limited even after long dwell time.

X-ray diffraction patterns of dense compacts (>0.98 TD) sintered under SSS and TSS3 schedule are shown in Fig. 10. For the specimen sintered under SSS condition at 1500 °C (grain size of 275 nm), both tetragonal and monoclinic phases were detected. The peak analysis (Eq. (1)) revealed the presence of approximately 3 wt.% monoclinic phase. No XRD peaks of the monoclinic phase were observed in the sintered specimen under TSS3 schedule (grain size of 110 nm). Full stabilization of the tetragonal zirconia ceramics at a critical grain size has been reported previously. For example, Lange[33] showed full stabilization in ZrO_2–3 mol% Y_2O_3 ceramic at the grains smaller than 0.8 μm; Winnubst and Burggraaf[34] reported the value of 0.25 μm for this ceramic in humid atmosphere; Theunissen et al.[22] stated the critical grain size to be 0.1, 0.4 and 2 μm for 6.8, 9 and 12 mol% Ce-PSZ, respectively. Therefore, in consistent with the result of previous researches it can stated that the critical grain size in 3Y-TZP should be <275 nm.

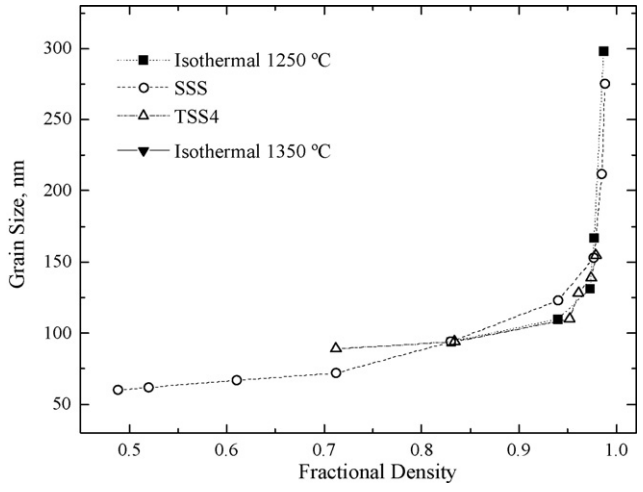

Fig. 9. Grain size-density curves obtained by single-step sintering (SSS) at various temperatures range between 1100 and 1500 °C, two-step sintering according to TSS4 cycle, and isothermal sintering at 1250 and 1350 °C for various times up to 8 h.

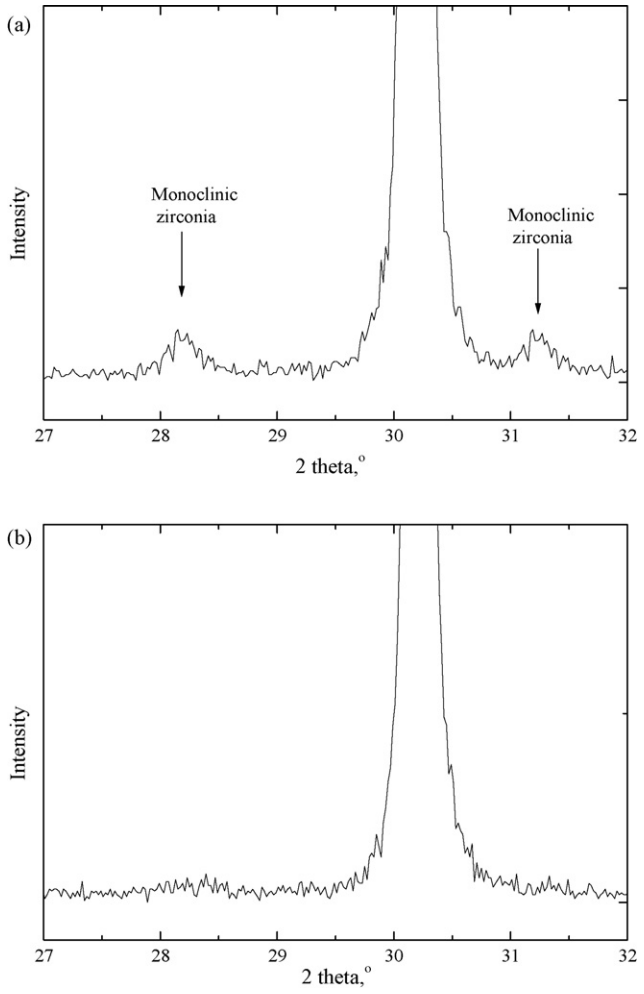

Fig. 10. XRD patterns of sintered 3Y-TZP: (a) single-step sintering at 1500 °C for 1 min; (b) two-step sintering according to TSS3 schedule.

4. Conclusion

The effect of TSS on the densification and grain growth of nanocrystalline 3Y-TZP ceramic was investigated. The findings can be summarized as following.

1. The grain growth rate of nanocrystalline 3Y-TZP in conventional sintering route is significantly lower than that of other ceramics such as ZnO and Al_2O_3. Full density compacts

with ultrafine grain structure (275 nm) can be obtained by single-step sintering.
2. To further decrease the grain growth rate, two-step sintering can be used. It was shown that the critical density which densification can proceeds without remarkable grain growth is 83% TD. The pore instability at this density level is obtained by 1 min firing at 1300 °C at the heating rate of 5 °C min^{-1}.
3. Full density compacts with an average grain size of 110 nm can be synthesized by firing at 1150 °C for 30 h after attending the critical density of 83% TD at the high temperature.
4. Full stabilized tetragonal zirconia (3Y-TZP) ceramic can be obtained at grain size <275 nm.

References

1. Subaro, E. C., *Science and Technology of Zirconia: Advanced in Ceramics*. ACERS Publisher, USA, 1981.
2. Gravie, R. C., Hannink, R. H. and Pascoe, R. T., Ceramic steel? *Nature*, 1975, **258**, 703–704.
3. Nieh, T. G. and Wadsworth, J., Superelastic behaviour of a fine-grained, yttria-stabilized, tetragonal zirconia polycrystal (Y-TZP). *Acta Materialia*, 1990, **38**, 1121–1133.
4. Mayo, M. J., Suresh, A. and Porter, W. D., Thermodynamics for nanosystems: grain and particle size dependent phase diagram. *Reviews on Advanced Materials Science*, 2003, **5**, 100–109.
5. Bowen, P. and Carry, C., From powders to sintered pieces: Formation, transformation and sintering of nanostructured ceramic oxides. *Powder Technology*, 2002, **128**, 248–255.
6. Wang, J. and Gao, L., Photoluminescence properties of nanocrystalline ZnO ceramics prepared by pressureless sintering and spark plasma sintering. *Journal of the American Ceramic Society*, 2005, **88**, 1637–1639.
7. Weibel, A., Bouchet, R., Denoyel, R. and Knauth, P., Hot pressing of nanocrystalline TiO_2 (anatase) ceramics with controlled microstructure. *Journal of European Ceramic Society*, 2007, **27**, 2641–2646.
8. Basu, B., Lee, J.-H. and Kim, D.-Y., Development of nanocrystalline wear-resistant Y-TZP ceramics. *Journal of the American Ceramic Society*, 2004, **87**, 1771–1774.
9. Dobedoe, R. S., West, G. D. and Lewis, M. H., Spark plasma sintering of ceramics. *Bulletin of the European Ceramic Society*, 2003, **1**, 19–24.
10. Krell, A. and Blank, P., The influence of shaping method on the grain size dependence of strength in dense submicrometer alumina. *Journal of the American Ceramic Society*, 1996, **16**, 1189–1200.
11. Duran, P., Vilegas, M., Capel, F. and Moure, C., Low-temperature sintering and microstructural development of nanocrystalline Y-TZP powder. *Journal of European Ceramic Society*, 1996, **16**, 945–952.
12. Chen, I. W. and Wang, X. H., Sintering dense nanocrystalline ceramics without final stage grain growth. *Nature*, 2000, **404**, 168–171.
13. Wang, X.-H., Chen, P.-L. and Chen, I.-W., Two-step sintering of ceramics with constant grain-size, I: Y_2O_3. *Journal of the American Ceramic Society*, 2006, **89**, 431–437.
14. Mazaheri, M., Zahedi, A. M. and Sadrnezhaad, S. K., Two-step sintering of nanocrystalline ZnO compacts: effect of temperature on densification and grain growth. *Journal of the American Ceramic Society*, 2008, **91**, 56–63.
15. Wang, X.-H., Deng, X. Y., Bai, H.-L., Zhou, H., Qu, W.-G., Li, L. T. and Chen, I.-W., Two-step sintering of ceramics with constant grain-size, II: $BaTiO_3$ and Ni–Cu–Zn ferrite. *Journal of the American Ceramic Society*, 2006, **90**, 438–443.
16. Bodisova, K. and Sajgalik, P., Two-stage sintering of alumina with submicrometer grain size. *Journal of the American Ceramic Society*, 2007, **90**, 330–332.
17. Lee, Y.-I., Kim, Y.-W., Mitomo, M. and Kim, D.-Y., Fabrication of dense nanostructured silicon carbide ceramics through two-step sintering. *Journal of the American Ceramic Society*, 2003, **86**, 1803–1805.
18. Duran, P., Capel, F., Tartaj, J. and Moure, C., A strategic two-stage low-temperature thermal processing leading to fully dense and fine-grained doped ZnO varisotors. *Advanced Materials*, 2002, **14**, 137–141.
19. Yu, P. C., Li, Q. F., Fuh, J. Y. H., Li, T. and Lu, L., Two-stage sintering of nano-sized yttria stabilized zirconia process by powder injection moulding. *Journal of Materials Processing Technology*, 2007, **192–193**, 312–318.
20. Lee, S.-Y., Sintering behavior and mechanical properties of injection-molded zirconia powder. *Ceramics International*, 2004, **30**, 579–584.
21. Cullity, B. D., *Elements of X-Ray Diffraction* (*2nd ed.*). Addison-Wesley Publishing Company Inc., Massachusetts, 1978.
22. Theunissen, G. S. A. M., Winnubst, A. J. A. and Burggraaf, A. J., Effect of dopants on the sintering behaviour and stability of tetragonal zirconia ceramics. *Journal of the European Ceramic Society*, 1992, **9**, 251–263.
23. Theunissen, G. S. A. M., Winnubst, A. J. A. and Burggraaf, A. J., Sintering kinetics and microstructure development of nano scale Y-TZP ceramics. *Journal of European Ceramic Society*, 1993, **11**, 315–324.
24. Mendelson, M. I., Average grain size in polycrystalline ceramics. *Journal of the American Ceramic Society*, 1969, **52**, 443–446.
25. Shi, J. L., Gao, J. H., Lin, Z. X. and Yan, D. S., Effect of agglomerates in ZrO_2 powder compacts on microstructural development. *Journal of Material Science*, 1993, **28**, 342–348.
26. Luo, J., Adak, S. and Stevens, R., Microstructure evolution and grain growth in the sintering of 3Y-TZP ceramics. *Journal of Material Science*, 1998, **33**, 5301–5309.
27. Ghosh, A., Suri, A. K., Rao, B. T. and Ramamohan, T. R., Low-temperature sintering and mechanical property evaluation of nanocrystalline 8 mol% yttria fully stabilized zirconia. *Journal of the American Ceramic Society*, 2007, **90**, 2015–2023.
28. Rahaman, M. N., *Sintering Technology, Sintering and Grain Growth of Ultra Fine Ceramics Powder*. Markel Dekker, UK, 1991.
29. Gao, L. and Li, W., Compacting and sintering behavior of nano ZrO_2 powders. *Scripta Materialia*, 2001, **44**, 2269–2272.
30. Mazaheri, M., Simchi, A., Dourandish, M. and Golestani-Fard, F., Master sintering curves of a nanoscale 3Y-TZP powder compacts. *Ceramics International*, 2008, doi:10.1016/j.ceramint.2008.01.008.
31. Li, J. and Ye, Y., Densification and grain growth of Al_2O_3 nanoceramics during pressureless sintering. *Journal of the American Ceramic Society*, 2006, **89**, 139–143.
32. Kang, S.-J. L., *Sintering Densification, Grain Growth and Microstructure*. Elsevier, Oxford, 2005.
33. Lange, F. F., Transformation toughening: experimental observation in the ZrO_2-Y_2O_3 system. *Journal of Material Science*, 1982, **17**, 240–246.
34. Winnubst, A. J. A. and Burggraaf, A. J., *Science and Technology of Zirconia III*. The American Cermaic Society Inc., Ohio, 1998.